Adipocyte Dynamics and Reversible Metabolic Syndrome in Mice with an Inducible Adipocyte-Specific Deletion of the Insulin Receptor

Supplemental Experimental Procedures and References

Supplemental Table 1

Supplemental Figures 1-7

Supplemental Figure Legends

Masaji Sakaguchi[1], Shiho Fujisaka[1], Weikang Cai[1], Jonathon N. Winnay[1], Masahiro Konishi[1], Brian O'Neill[1], Mengyao Li[1], Rubén García-Martín[1], Hirokazu Takahashi[1], Jian Hu[2], Rohit N. Kulkanri[2] and C. Ronald Kahn[1*]

[1]Section of Integrative Physiology and Metabolism and [2]Section of Islet Cell & Regenerative Biology,

Joslin Diabetes Center, Harvard Medical School, Boston, MA 02215, USA

*Address correspondence to:

C. Ronald Kahn, M.D

Fax: (617) 309-2593

E-mail: c.ronald.kahn@joslin.harvard.edu

Supplemental Experimental Procedures

Animal Studies

Male mice were used for all studies unless otherwise indicated. Adiponectin-CreERT2 mice were a generous gift from the Stefan Offermans (Max-Planck-Institute for Heart and Lung Research, Bad Nauheim, German) and can now be purchased at Jackson Laboratories (stock no. 025124). IR and IGF1R floxed mice have been described previously (Boucher et al., 2012). Control and fat-specific inducible IGF1R KO (Ai-IGFRKO), IR KO (Ai-IRKO) and double KO (Ai-DKO) mice were maintained on a mixed (C57Bl/6 – 129Sv) background by breeding Adiponectin-CreERT2 IRf/f and/or IGF1Rf/f with IRf/f and/or IGF1Rf/f mice. For induction of recombination, mice were treated with 100 mg/kg tamoxifen (Sigma) dissolved in 10% ethanol and 90% peanut oil (Sigma) by intraperitoneal injection five times over a six-day period starting at 7 weeks of age. In these experiments, tamoxifen was given to all animal groups including control mice, which carried the floxed alleles, but lacked the Adiponectin-CreERT2 transgene. All mice were maintained on a normal chow diet (Mouse diet 9F 5020; PharmaServ).

Histopathology and immunohistochemistry

The average percentage of TUNEL+/DAPI+ double-positive cells was quantified from five fields using 20x microscope objective. 3 sections per mouse fat pad from the subcutaneous white fat and interscapular brown fat (4-6 animals per group) were examined. Quantification of cleaved caspase-3 positive cells/high power field (hpf) was performed using 40x microscope objective in a similar manner. The confirmation that the staining was in adipocytes was based on the morphology as described. Also by lineage tracing experiments, the lost cells were adipocytes as shown in Figures 4D, 5C, S4G and S5B. To assess hepatic steatosis, frozen liver sections fixed with 10% buffered formalin for 30 min at room temperature and stained for 7 min with a filtered solution of 0.7% Oil Red O in propylene glycol, and counterstained with hematoxylin for 1 min, washed 3 times with distilled water, and then visualized. 3 sections of 3 livers were assessed for each genotype.

Body temperature and cold exposure

For cold exposure, mice were housed individually and subjected to a cold room at 8 °C for up to 3 hours. During this period, mice were without access to food or water. The rectal temperature was assessed using a RET-3 rectal probe (Physitemp) at the time before and after exposure (30, 60, 90, 120, 150 and 180 minutes) to the cold, then mice were re-warmed using a heating pad. All mice recovered and were healthy. Skin temperature over BAT was also measured using a thermal imaging camera (FLIR T300 Infrared Camera) without anesthesia and analyzed using appropriate software (FLIR Tools Software).

Quantitative RT-PCR

Real-time PCR was performed using SYBR Green (Bio-Rad) with specific primers on an ABI Prism 7900HT sequence (Applied Biosystems) with primers shown in Supplementary Table 1. All expression data were normalized to TATA-binding protein expression using the relative standard curve method.

β-cell histology and proliferation

The methods used for analyses have been described previously (Kulkarni et al., 1999; Okada et al., 2007). Briefly, for quantification of β-cell proliferation paraffin embedded pancreas sections were co-immunostained with Ki67 (BD) and insulin (Abcam) followed by incubation with the secondary antibody conjugated with Alexa 488 and 594 (Jackson Immuno Research). Images were recorded using a fluorescence microscope at 20x magnification and cell counting was performed using Image J software (Rasband, W.S., 1997-2009). For each sample, at least 1000-3000 beta cells (insulin positive cells) were counted in a blinded manner by a single person, and the number of Ki67 positive cells were recorded. The percentage of Ki67 positive cells was calculated using the formula: (number of Ki67/insulin double + cells / total number of insulin + cells) x 100%. For measurement of β-cell mass, mouse pancreas tissue was fixed in formaldehyde and embedded in paraffin. Five micron sections of pancreas were cut and immunostained using insulin antibody (Abcam), followed by incubation with the secondary antibody conjugated with Alexa 594 (Jackson Immuno Research). Images were captured using fluorescence microscope. Each slide was captured under both 4x and 20x magnifications for the whole pancreas and individual islets. Images were analyzed using Image J software. The beta cell mass was calculated by using the formula: (β-cell area / pancreas area) x pancreatic weight (mg).

White and brown preadipocytes isolation and culture

Preadipocyte cell lines were generated as described previously (Boucher et al., 2010). Briefly, preadipocytes were isolated from intrascapular brown adipose tissue of newborn control mice or intra-abdominal white adipose tissue of 8-week-old control mice. Each fat pad was digested with type II collagenase (Sigma) for 40 min at 37 °C and immortalized by infection with retrovirus encoding SV40 T-antigen as previously described, followed by the selection with 2 μg/ml of puromycin. Immortalized preadipocytes and 3T3-L1 cells were maintained in DMEM supplemented with 10% heat-inactivated FBS, 100 U/ml penicillin and 100 μg/ml streptomycin, and cultured at 37 °C in a humidified atmosphere of 5% CO_2. Brown preadipocytes differentiation was induced with an induction mixture containing 20 nM insulin and 1 nM triiodothyronine, 0.5 mM isobutylmethylxanthine, 1 μM dexamethasone, and 0.125 mM indomethacin for 48 h. White preadipocyte differentiation was induced with 100 nM insulin, 0.5 mM isobutylmethylxanthine, 1 μM dexamethasone and 1 μM troglitazone. Media with or

without leptin (0, 1, 5, 10, 20 and 100 nM) were changed every 2 days. Lipid accumulation was visualized at day 8 by oil red O staining.

Adipocyte cell size

Tissues were fixed overnight with neutral-buffered 10% formalin at 4°C, paraffin embedded, sectioned, and stained with hematoxylin and eosin. Adipocyte area was determined by quantifying the adipocyte area of a total of ~20,000 cells from 4 animals per study group using Adiposoft image analysis software.

Supplemental References

Boucher, J., Tseng, Y.H., and Kahn, C.R. (2010). Insulin and insulin-like growth factor-1 receptors act as ligand-specific amplitude modulators of a common pathway regulating gene transcription. J Biol Chem 285, 17235-17245.

Boucher, J., Mori, M.A., Lee, K.Y., Smyth, G., Liew, C.W., Macotela, Y., Rourk, M., Bluher, M., Russell, S.J., and Kahn, C.R. (2012). Impaired thermogenesis and adipose tissue development in mice with fat-specific disruption of insulin and IGF-1 signalling. Nat Commun 3, 902. doi: 10.1038/ncomms1905.

Kulkarni, R. N., Bruning, J. C., Winnay, J. N., Postic, C., Magnuson, M. A., and Kahn, C. R. (1999). Tissue-specific knockout of the insulin receptor in pancreatic beta cells creates an insulin secretory defect similar to that in type 2 diabetes. Cell *96*, 329-339.

Okada, T., Liew, CW., Hu, J., Hinault, C., Michael, MD., Krtzfeldt, J., Yin, C., Holzenberger, M., Stoffel, M., and Kulkarni RN. (2007). Insulin receptors in beta-cells are critical for islet compensatory growth response to insulin resistance. Proc Natl Acad Sci U S A *104,* 8977-8982

Rasband, W.S., ImageJ, U. S. National Institutes of Health, Bethesda, Maryland, USA, http://rsb.info.nih.gov/ij/, 1997-2009

Table S1 (related to all Figures). Quantitative Real-Time PCR primer sequences

Gene	Direction	Sequence
TBP	Forward	ACCCTTCACCAATGACTCCTATG
TBP	Reverse	TGACTGCAGCAAATCGCTTGG
FAS	Forward	GAGGACACTCAAGTGGCTGA
FAS	Reverse	GTGAGGTTGCTGTCGTCTGT
AP2	Forward	GATGCCTTTGTGGGAACCT
AP2	Reverse	CTGTCGTCTGCGGTGATTT
HSL	Forward	ACGGATACCGTAGTTTGGTGC
HSL	Reverse	TCCAGAAGTGCACATCCAGGT
ATGL	Forward	ACTGTGGCCTCATTCCTCCT
ATGL	Reverse	AACTGGATGCTGGTGTTGGT
Adiponectin	Forward	GATGGCACTCCTGGAGAGAA
Adiponectin	Reverse	GCTTCTCCAGGCTCTCCTTT
Leptin for	Forward	GGGCTTCACCCCATTCTGA
Leptin rev	Reverse	TGGCTATCTGCACATTTTG
Glut4	Forward	ATCTTGATGACCGTGGCTCT
Glut4	Reverse	CTCAAAGAAGGCCACAAAGC
PPAR γ	Forward	TGTTATGGGTGAAACTCTGGG
PPAR γ	Reverse	AGAGCTGATTCCGAAGTTGG
Elovl3	Forward	GGACTTAAGGCCCTTTTTGG
Elovl3	Reverse	TTCCGCGTTCTCATGTAGGT
Cidea	Forward	ATCACAACTGGCCTGGTTACG
Cidea	Reverse	TACTACCCGGTGTCCATTTCT
Shox2	Forward	TGGAACAACTCAACGAGCTGGAGA
Shox2	Reverse	TTCAAACTGGCTAGCGGCTCCTAT
Tmem26	Forward	TTCCTGTTGCATTCCCTGGTC
Tmem26	Reverse	GCCGGAGAAAGCCATTTG
Glut2	Forward	AGCTCCCTGGGATGAAGAG
Glut2	Reverse	ATCAAGAGGGCTCCAGTCAA
SREBP1c	Forward	ATCTCCTAGAGCGAGCGTTG
SREBP1c	Reverse	TATTTAGCAACTGCAGATATCCAA
FBP1	Forward	CCATCATAATCGAACCTGAG
FBP1	Reverse	CTTCTCAGAAGGCTCATCAG
SerpinB1	Forward	GCTGCTACAGGAGGCATTGC
SerpinB1	Reverse	CGGATGGTCCACTGTGAATTC
Betatrophin	Forward	GTACGGAGACTACAAGTGCAG
Betatrophin	Reverse	CCAGTGAGAGCCCATAAGAG
UCP1	Forward	ACTGCCACACCTCCAGTCATT
UCP1	Reverse	CTTTGCCTCACTCAGGATTGG
Adrb3	Forward	GCTGACTTGGTAGTGGGACTC
Adrb3	Reverse	TAGAAGGAGACGGAGGAGGAG
PRDM16	Forward	CAGCACGGTGAAGCCATTC
PRDM16	Reverse	GCGTGCATCCGCTTGTG
PGC1 α	Forward	CCCTGCCATTGTTAAGACC
PGC1 α	Reverse	TGCTGCTGTTCCTGTTTTC
CEBP α	Forward	CAAGAACAGCAACGAGTACCG
CEBP α	Reverse	GTCACTGGTCAACTCCAGCAC
Tfam	Forward	AGTTCCCACGCTGGTAGTGT
Tfam	Reverse	GCGCACATCTCGACCC

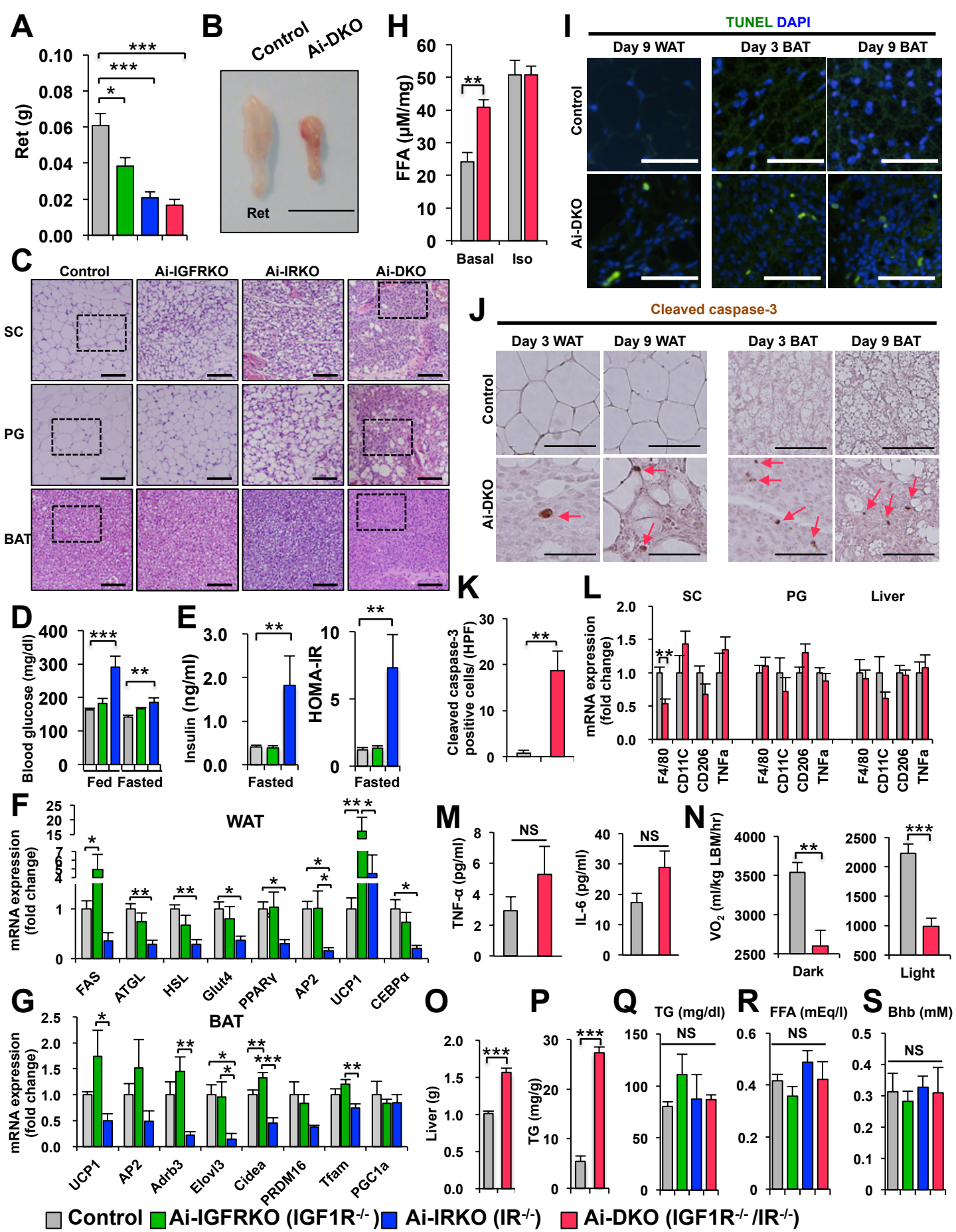

Figure S1 (related to Figure 1)

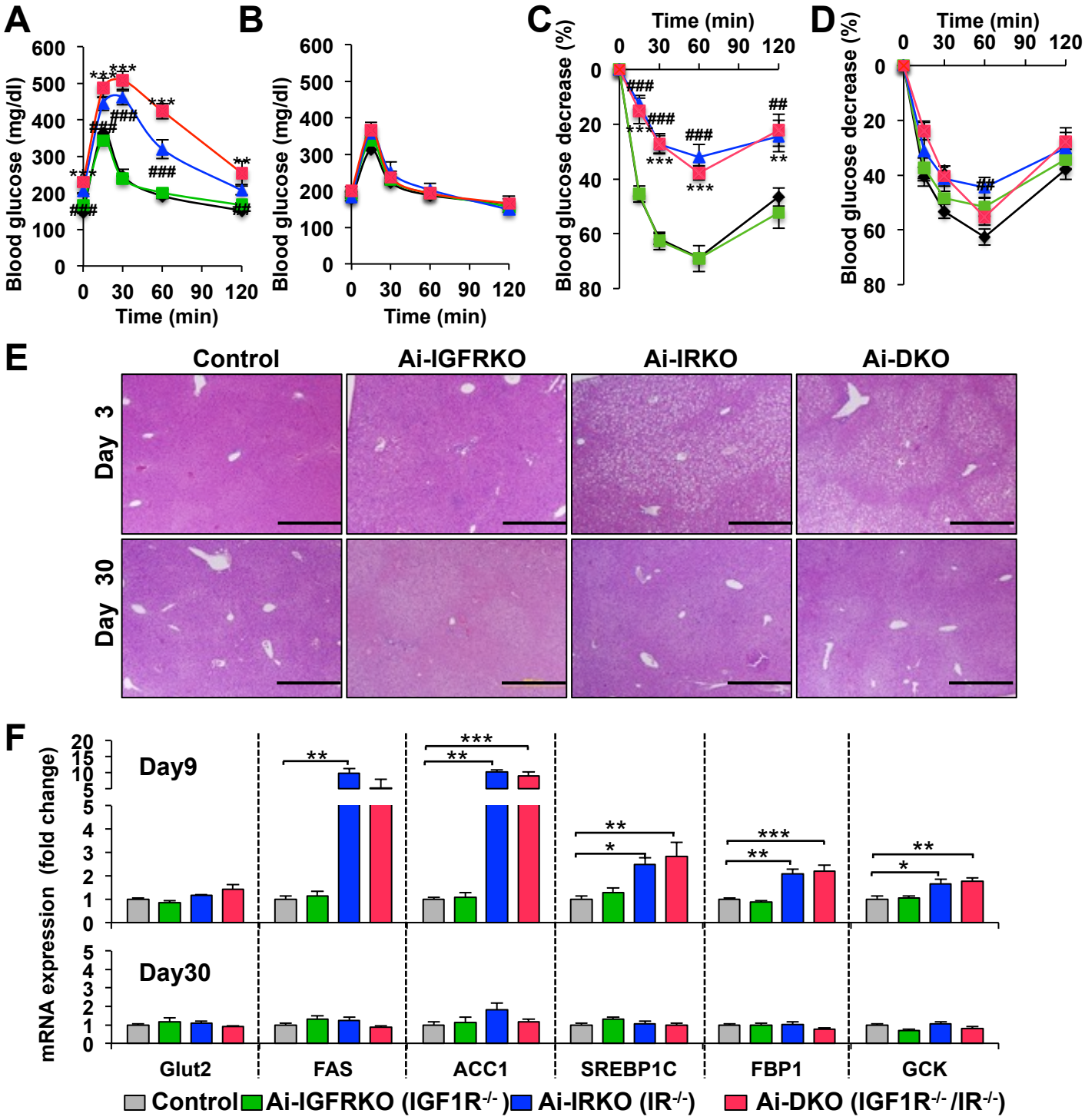

Figure S2 (related to Figure 2)

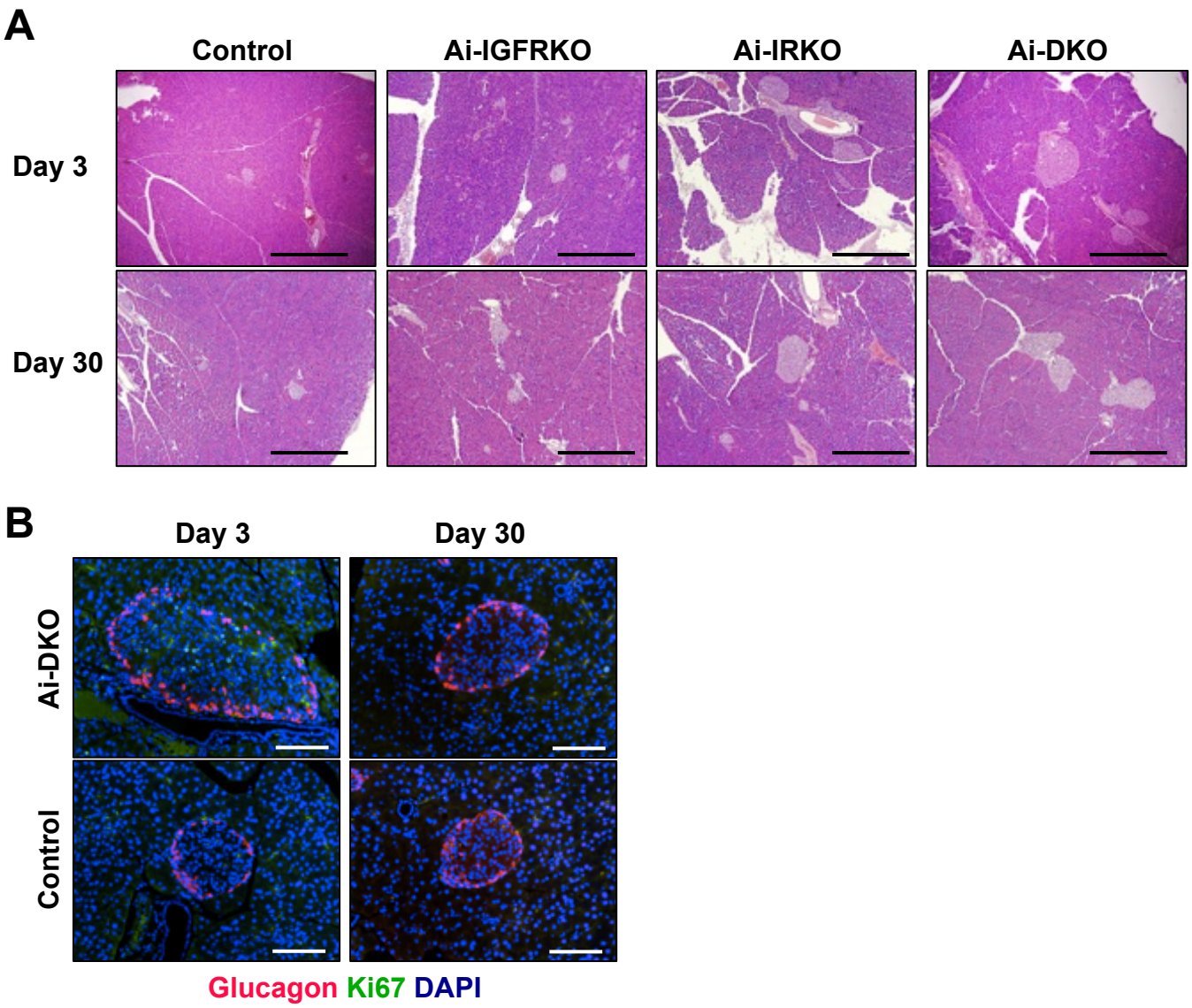

Figure S3 (related to Figure 3)

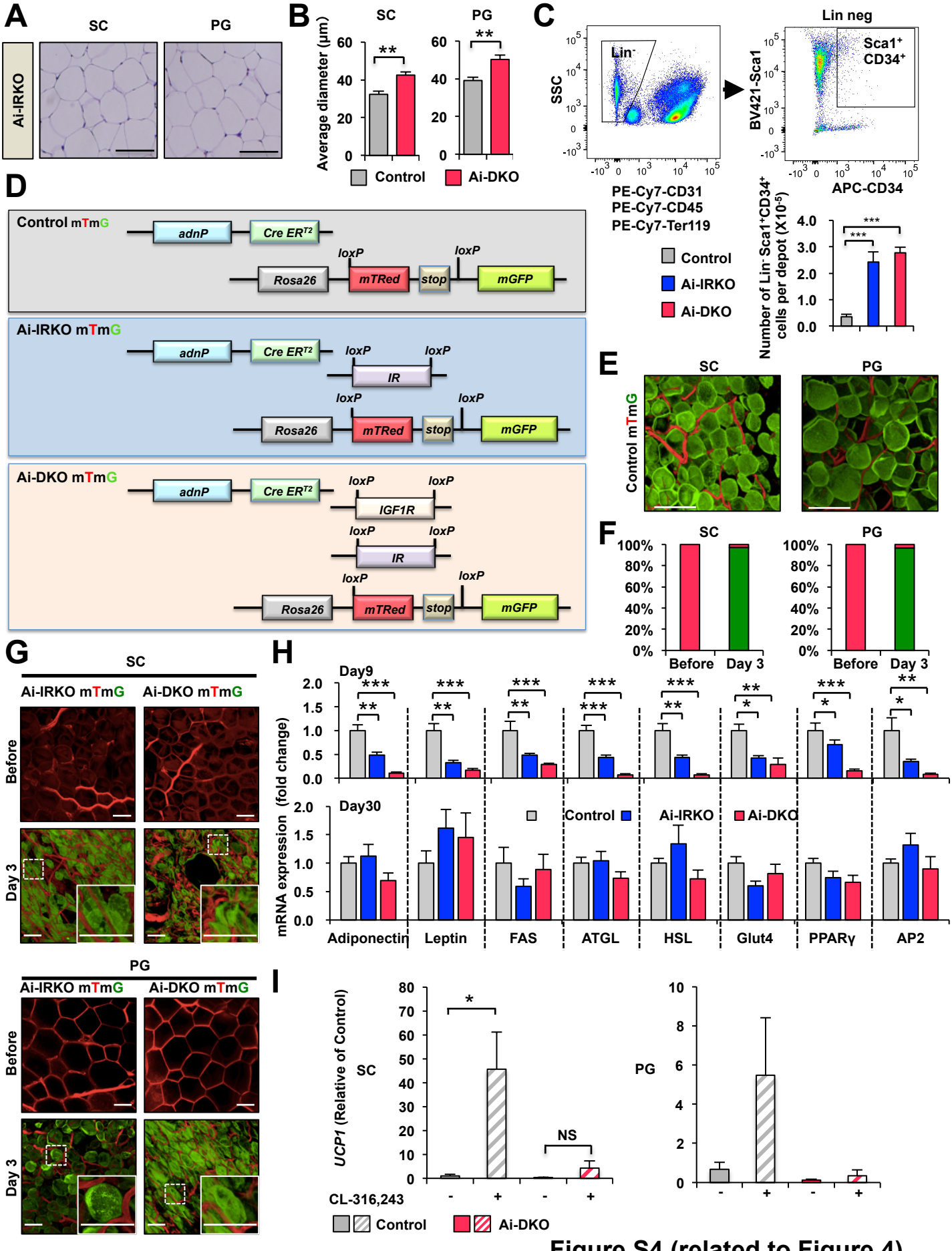

Figure S4 (related to Figure 4)

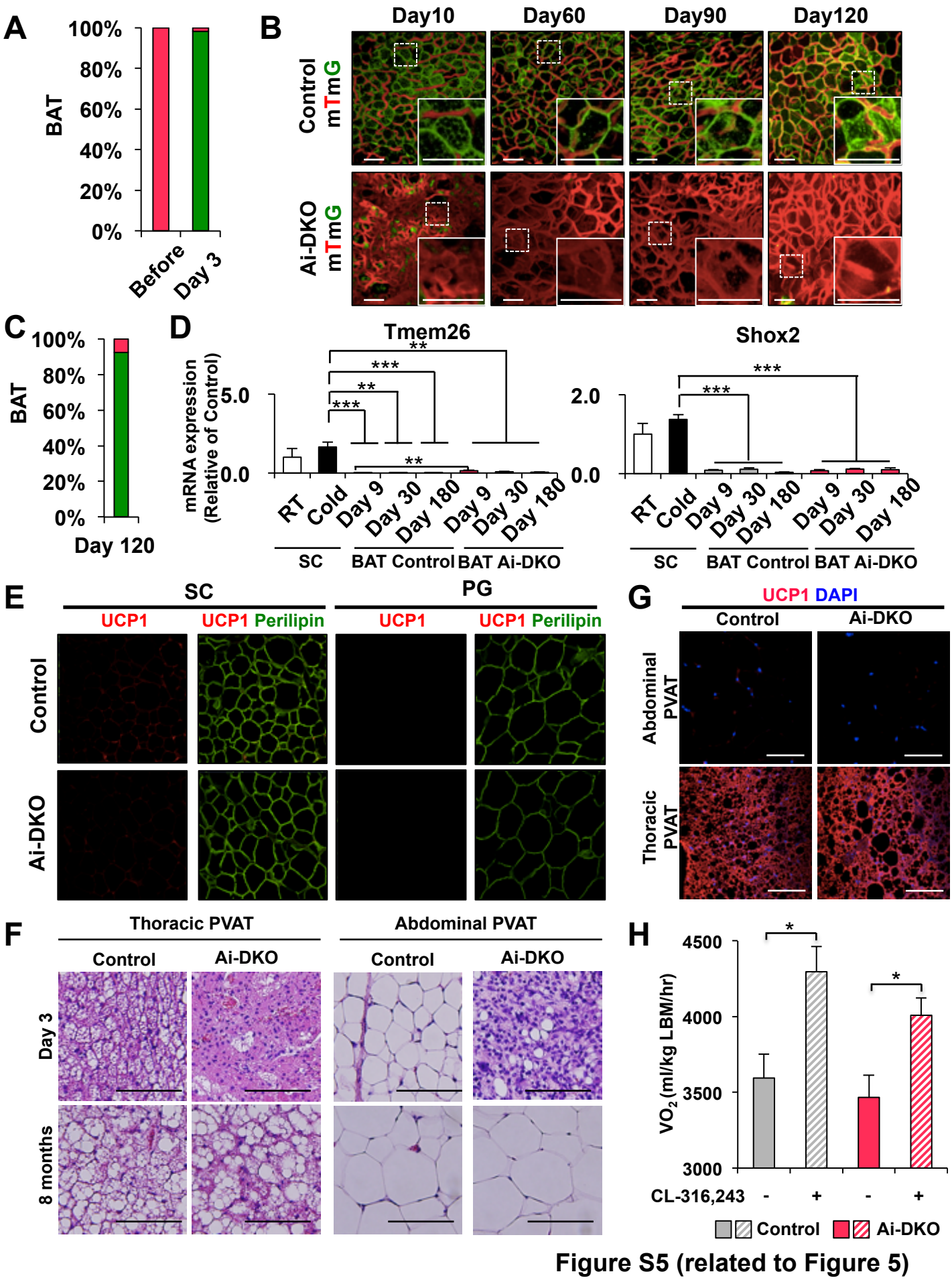

Figure S5 (related to Figure 5)

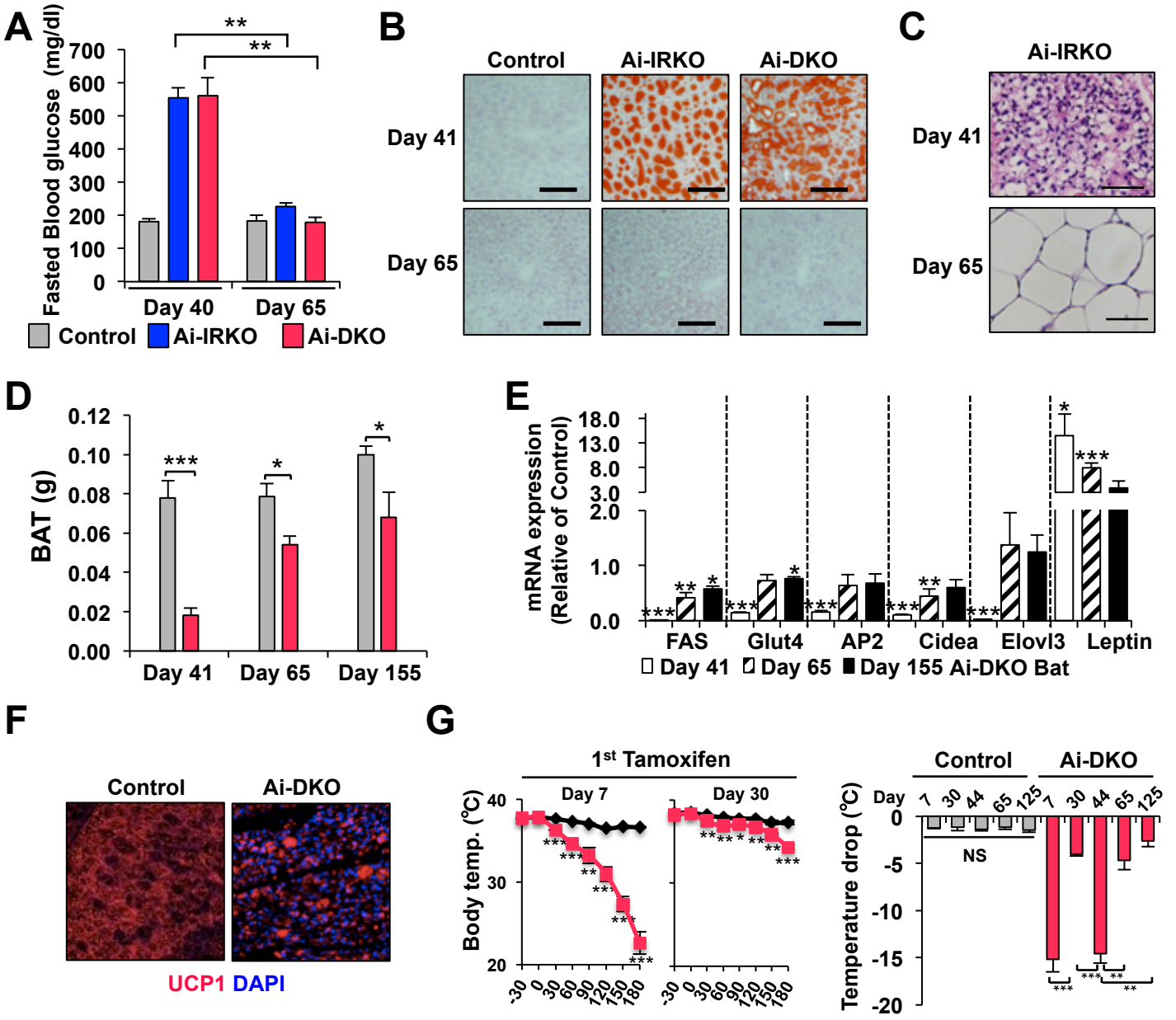

Figure S6 (related to Figure 6)

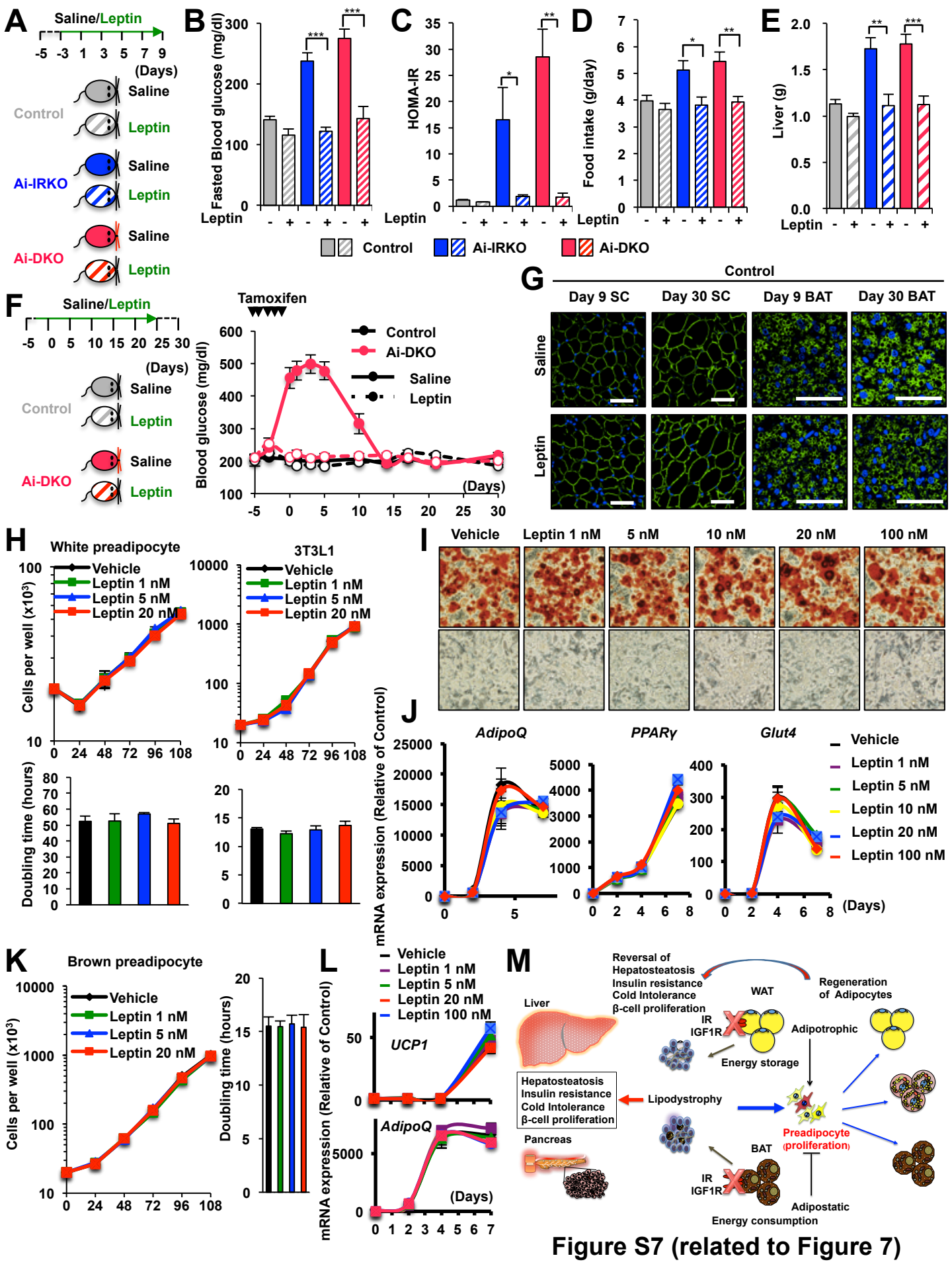

Figure S7 (related to Figure 7)

Supplemental Figure Legends

Figure S1 (related to main Figure 1). Effects of acute disruption of IR or/and IGF1R in fat tissues of adult mice. (**A**) Tissue weights of retroperitoneal depot weights in Control (*n* = 13), Ai-IGFRKO (*IGF1R-/-*) (*n* = 6), Ai-IRKO (*IR-/-*) (*n* = 13) and Ai-DKO (*IGF1R-/- IR-/-*) (*n* = 12) male mice at day 3 after treatment with tamoxifen under chow diet feeding. (**B**) Comparison of retroperitoneal adipose tissues between Control and Ai-DKO mice at day 3. Representative pictures are shown. Scale bars, 1 cm. (**C**) Histological analysis of adipose tissues with hematoxylin and eosin (H & E) staining. Sections of BAT and WAT (SC and PG) were examined in Control, Ai-IGFRKO, Ai-IRKO and Ai-DKO mice at day 3. Scale bars, 50 μm. (**D**) Comparison of blood glucose levels between Control (*n* = 13), Ai-IGFRKO (*n* = 7) and Ai-IRKO (*n* = 6) under fed and fasted conditions at day 2. (**E**) Serum insulin and HOMA-IR levels of Control (*n* = 13) Ai-IGFRKO (*n* = 7) and Ai-IRKO (*n* = 6) under fasting conditions at day 2. (**F**) Levels of mRNA measured by real-time PCR in WAT (SC) from Control, Ai-IGFRKO and Ai-IRKO at day 3. (*n* = 5-7 per group) (**G**) mRNA abundance measured by real-time PCR in BAT from Control, Ai-IGFRKO and Ai-IRKO at day 3 (*n* = 5-7 per group). (**H**) Lipolysis assessed by FFA release from PG-WAT of Control (*n* = 6) and Ai-DKO (*n* = 8) at day 1.5. Samples were incubated *ex vivo* for 2 h at 37 °C in the presence or absence of 10 μM isoprenaline, and FFA released into the medium was quantified. (**I**) SC-WAT and BAT sections were stained for TUNEL and DAPI in Control and Ai-DKO mice at day 3 and day 9. (**J**) SC-WAT and BAT sections were immunostained for cleaved caspase-3 in Control and Ai-DKO mice at day 3 and 9 (bottom). Scale bars, 100 mm. (**K**) Quantification of cleaved caspase-3 positive measured as cells/high power field (hpf) at day 3 in SC. (*n* = 4-6 per group) (40x microscope objective) (**L**) Expression levels of mRNA measured by real-time qPCR in SC, PG and Liver from Control and Ai-DKO at day 3 (*n* = 5-7 per group). (**M**) Serum TNF-α and IL-6 concentrations at day 3. (*n* = 5/genotype) (**N**) Oxygen consumption (VO_2) measured in metabolic cages with Control (*n* = 6) and Ai-DKO (*n* = 6) mice 1 week after treatment with tamoxifen. (**O**) Liver weights in Control (gray, *n* = 12) and Ai-DKO (red, *n* = 12) at day 3. (**P**) TG concentrations in livers of Control (*n* = 7) and Ai-DKO (*n* = 6) mice fasted for 6 h on day 3 post tamoxifen-treatment (right). (**Q**) Serum TG (*n* = 6-7 per group), (**R**) FFA (*n* = 6-8 per group) and (**S**) Bhb concentrations at day 2. (*n* = 5/each) Statistical significance is shown as $p<0.05$ (*), $p<0.01$ (**), and $p<0.001$ (***).

Figure S2 (related to main Figure 2). Ai-IRKO and Ai-DKO show acute insulin resistance which improved after 1 month. (**A**) Comparison of GTT in all groups at day 2 and day 30 (**B**) after treatmentwith tamoxifen. (**C**) Comparison of GTT in all groups at day 2 and at day 30 (**D**). Control (black), Ai-IGFRKO (green), Ai-IRKO (blue) and Ai-DKO (red). (**E**) Liver tissue sections stained with H & E at day 3 and day 30. Scale bars, 500 μm. High magnification pictures in Control and Ai-DKO were shown in **Figure 1N**. (**F**) Expression levels of mRNA measured by real-time PCR in livers from Control, Ai-IGFRKO, Ai-IRKO and Ai-DKO at days 9 and 30 (*n* = 5-7 per group). Statistical significance is shown as $p<0.05$ (*), $p<0.01$ (**), and $p<0.001$ (***). NS (not significant) suggests no change.

Figure S3 (related to main Figure 3). Ai-DKO induces acute pancreatic β-cell proliferation and increase in b-cell mass. (**A**) Pancreas tissue sections at day 3 and day 30. Scale bars, 500 mm. (**B**) Pancreatic sections were immunostained for glucagon and Ki67 in Control and Ai-DKO mice at day 3 and day 30 after tamoxifen treatment. Scale bars, 100 mm.

Figure S4 (related to main Figure 4). Adipose tissue biology of SC and PG fat in Control, Ai-IRKO and Ai- DKO mice. (**A**) SC and PG sections were with H&E in Ai-IRKO mice at day 30. Scale bars, 50 μm. (**B**) Average adipocyte diameter in SC (upper) and PG adipocytes (bottom) (*n* = 4 per group). (**C**) PI- negative singlet cells were sorted for lack of CD31, CD45 and Ter119 expression (Lin-) (**upper left**) and were then sorted on the basis of expression of Sca1 and CD34 (**upper right**). Representative Sca1+ and CD34+ gates used for sorting are indicated. Quantification of the Lin- Sca1+CD34+ cells from SC-WAT per depot at day 3 (**lower panel**). (*n* = 6-11 per group) (**D**) Strategy for identifying newly developed adipocytes in Ai-IRKO and Ai-DKO mice in combination of floxed *mTmG* mouse. (**E**) Inducible labeling of mature SC and PG adipocytes in Control at day 3 after tamoxifen- treatment. (**F**) Percentage of mTFP+ and mGFP+ adipocytes from each of the depots in Control before and day 3 after tamoxifen-treatment (*n* = 3). (**G**) Lineage tracing of mature SC and PG adipocytes in Ai-IRKO and Ai-DKO before and after tamoxifen treatment at day 3. (**H**) The relative mRNA levels of PG adipocytes in Ai-IRKO (*n* = 6) and Ai-DKO (*n* = 6) from day 9 to day 30 after tamoxifen treatment compared with Controls (*n* = 7) defined as 1.0. (**I**) qPCR of *Ucp1* gene expression in SC (**left**) and PG-WAT (**right**) from Control and Ai-DKO female mice treated with CL-316,243 (1 mg/kg) or vehicle for 7 days. (*n* = 4-8 per group) Results are expressed as fold change over the Control (vehicle) group. Statistical significance is shown as $p<0.05$ (*), $p<0.01$ (**) and $p<0.001$ (***). NS (not significant).

Figure S5 (related to main Figure 5). Brown adipocyte regeneration in Ai-DKO mice. (**A**) Percentage of mTFP+ and mGFP+ adipocytes in brown fat in Control before and day 3 after tamoxifen treatment (*n* = 3). (**B**) Inducible labeling of mature brown adipocytes in BAT of Control and Ai-DKO in combination with the *mTmG* transgene before and at days 10, 60, 90, and 120 after tamoxifen treatment. Scale bars, 50 μm. (**C**) Percentage of mTFP+ and mGFP+ adipocytes in brown fat in Control day 120 after tamoxifen-treatment (*n* = 3). (**D**) The relative mRNA levels of *Tmem26* (**left**) and *Shox2* (**right**), two beige adipocyte markers, were measured in SC adipose tissue from mice maintained at room temperature (RT) and 1 week after cold challenge (Cold) in Control and Ai- DKO BAT at days 9, 30 and 180 after tamoxifen treatment (*n* = 4-7 per group). (**E**) UCP1 expression in WAT (SC and PG) by anti-UCP1 immunostaining in Control and Ai-DKO at day 180 after tamoxifen-treatment. (**F**) Histological analysis of thoracic (**left**) and abdominal perivascular adipose tissues (**right**) following hematoxylin & eosin staining at day 3 and 8 months. Scale bars, 100 μm. (**G**) UCP1 expression in thoracic and abdominal perivascular adipose sections by anti- UCP1 immunostaining in Control and Ai-DKO

at 8 months after tamoxifen-treatment. (**H**) Oxygen consumption (VO2) of Control and Ai-DKO mice with a injection of CL-316,243 (1 mg/kg) or vehicle (n = 6 per group) 6 weeks after treatment with tamoxifen. Statistical significance is shown as $p<0.05$ (*), $p<0.01$ (**) and $p<0.001$ (***). NS (not significant).

Figure S6 (related to main Figure 6). Regeneration potential of WAT and BAT was preserved even after tamoxifen-treatment for second time. (**A**) Fasted blood glucose levels after 1st and 2nd treatment of tamoxifen. Blood glucose levels were measured in Control (n = 5), Ai-IRKO (n = 5) and Ai-DKO (n = 5) until day 65. (**B**) Liver tissue sections stained with Oil Red O in Control, Ai-IRKO and Ai-DKO at day 41 and day 65. Scale bars, 100 μm. (**C**) SC white adipose sections stained with H&E in Ai-IRKO mice at days 41 and 65. Scale bars, 50 μm. (**D**) Recovery of tissue weights of BAT in Ai-DKO male mice at days 41, 65 and 155 compared with Control (n = 5-10 per group). (**E**) The relative mRNA levels in Ai- DKO brown adipocytes compared with Controls at days 41, 65 and 155 after tamoxifen treatment (n = 5-10 per group). (**F**) UCP1 expression in BAT by anti-UCP1 immunostaining in Control and Ai-DKO at day 9. Scale bars, 50 μm. (**G**) Rectal temperature in male Control and Ai-DKO taken every 30 min for 3 h during exposure to an 8 °C environment (n=5 per group) at day 7 and day 30 (left). Comparison of rectal temperature drop after 3 h of 4 °C challenge in Control and Ai-DKO mice (right). Statistical significance is shown as $p<0.05$ (*), $p<0.01$ (**) and $p<0.001$ (***). NS (not significant).

Figure S7 (related to main Figure 7). Effects of leptin treatment in Ai-IRKO and Ai-DKO mice. (**A**) Leptin administered by Alzet mini-pump between day -3 and day 9 of tamoxifen treatment. (**B**) Fasted blood glucose was compared at day 3 after tamoxifen treatment (n = 5-6 per group). (**C**) Comparison of HOMA-IR levels (n = 5-6 per group). (**D**) Food intake (g) per day in all groups between day 0 and day 6 Ai-IRKO, Ai-DKO and Control (n = 5-6 per group). Leptin treatment normalized hyperphagia and food intake in Ai-IRKO and Ai-DKO. (**E**) Liver weights at day 9 after tamoxifen treatment in Ai-IRKO (Saline: n=6, leptin: n=5), Ai-DKO (Saline: n = 7, leptin: n = 6) and Control (Saline: n = 9, leptin: n = 7). (**F**) Continuous leptin administration was performed by Alzet mini pump (DURECT Corporation) between day -3 and day 25 post tamoxifen-treatment (**left)**. Fed glucose levels in Control with saline (n =7), Control with leptin (n = 6), Ai-DKO with saline (n = 5) and Ai-DKO with leptin (n = 5) mice before and after treatment of tamoxifen (**right**). (**G**) Perilipin (green) staining of SC and BAT in Control (with saline or leptin treatment) at day 9 and day 30 after tamoxifen treatment. Scale bars, 50 μm. (**H**) Effect of leptin on growth rate of white preadipocytes and 3T3-L1 cell lines *in vitro*. Cells were plated at a density of 20,000 cells per well and and their number determined at 24h intervals for 5 consecutive days (upper). Doubling time was calculated during the exponential growth phase between day 3 and day 4 after plating (**bottom**). (**I**) Oil Red O staining of white preadipocyte cells differentiated for 8 days in the absence or in the presence of leptin (1, 5,10, 20, 100 μM). Bright field microscopy picture of the differentiated cells are shown (**bottom**). (**J**) mRNA abundance was measured by real time PCR in white preadipocytes during the

differentiation process before or 2, 4 and 8 days after induction of the differentiation in the absence or in the presence of leptin (1, 5, 10, 20, 100 μM). Results are mean + SEM of 4 independent experiments. (**K**) Leptin treatment effects on growth rate in brown preadipocytes. Cells were plated at a density of 20,000 cells per well, and and their number determined at 24 h intervals for 5 consecutive days (**left**). Doubling time was calculated during the exponential growth phase between day 3 and day 4 after plating (**right)**. (**L**) mRNA abundance was measured by real time PCR in brown preadipocytes before or 2, 4 and 7 days after induction of the differentiation in the absence or in the presence of leptin (1, 5, 20, 100 μM). Results are mean + SEM. of 4 independent experiments. Statistical significance is shown as $p<0.05$ (*), $p<0.01$ (**) and $p<0.001$ (***). **(M)** Schematic model of the development and resolution of lipodystrophy and the metabolic syndrome following inactivation of the insulin and/or IGF-1 receptors on white and brown adipocytes.